

Chernina V. Yu.<sup>1</sup>, Pisov M. E.<sup>2</sup>, Belyaev M. G.<sup>2</sup>, Bekk I. V.<sup>3</sup>, Zamyatina K. A.<sup>4</sup>, Korb T. A.<sup>1</sup>, Aleshina O. O.<sup>1</sup>, Shukina E. A.<sup>5</sup>, Solovev A. V.<sup>6</sup>, Skvortsov R. A.<sup>3</sup>, Filatova D. A.<sup>7</sup>, Sitdikov D. I.<sup>8</sup>, Chesnokova A. O.<sup>8</sup>, Morozov S. P.<sup>1</sup>, Gombolevskiy V. A.<sup>1</sup>

<sup>1</sup> Research and Practical Clinical Center for Diagnostics and Telemedicine Technologies of the Moscow Health Care Department, Moscow, Russia

<sup>2</sup> Skolkovo Institute of Science and Technology, Moscow, Russia

<sup>3</sup> The Russian National Research Medical University named after N.I. Pirogov, Moscow, Russia

<sup>4</sup> A.V. Vishnevsky National Medical Research Center of Surgery, Moscow, Russia

<sup>5</sup> MSMSU after A.I. Evdokimov, Moscow, Russia

<sup>6</sup> Sklifosovsky Clinical and Research Institute for Emergency Medicine, Moscow, Russia

<sup>7</sup> Lomonosov Moscow State University, Moscow, Russia

<sup>8</sup> Sechenov First Moscow State Medical University, Moscow, Russia

## EPICARDIAL FAT TISSUE VOLUMETRY: COMPARISON OF SEMI-AUTOMATIC MEASUREMENT AND THE MACHINE LEARNING ALGORITHM

<i>Aim</i>	To compare assessments of epicardial adipose tissue (EAT) volumes obtained with a semi-automatic, physician-performed analysis and an automatic analysis using a machine-learning algorithm by data of low-dose (LDCT) and standard computed tomography (CT) of chest organs.
<i>Material and methods</i>	This analytical, retrospective, transversal study randomly included 100 patients from a database of a united radiological informational service (URIS). The patients underwent LDCT as a part of the project «Low-dose chest computed tomography as a screening method for detection of lung cancer and other diseases of chest organs» (n=50) and chest CT according to a standard protocol (n=50) in outpatient clinics of Moscow. Each image was read by two radiologists on a Syngo. via VB20 workstation. In addition, each image was evaluated with a developed machine-learning algorithm, which provides a completely automatic measurement of EAT.
<i>Results</i>	Comparison of EAT volumes obtained with chest LDCT and CT showed highly consistent results both for the expert-performed semi-automatic analyses (correlation coefficient >98%) and between the expert layout and the machine-learning algorithm (correlation coefficient >95%). Time of performing segmentation and volumetry on one image with the machine-learning algorithm was not longer than 40 sec, which was 30 times faster than the quantitative analysis performed by an expert and potentially facilitated quantification of the EAT volume in the clinical conditions.
<i>Conclusion</i>	The proposed method of automatic volumetry will expedite the analysis of EAT for predicting the risk of ischemic heart disease.
<i>Keywords</i>	Epicardial adipose tissue; computed tomography; volumetry; machine-learning algorithm; low-dose computed tomography
<i>For citation</i>	Chernina V. Yu., Pisov M. E., Belyaev M. G., Bekk I. V., Zamyatina K. A., Korb T. A. et al. Epicardial fat Tissue Volumetry: Comparison of Semi-Automatic Measurement and the Machine Learning Algorithm. <i>Kardiologiya</i> . 2020;60(9):46–54. [Russian: Чернина В.Ю., Писов М.Е., Беляев М.Г., Бекк И.В., Замятина К.А., Корб Т.А. и др. Волюметрия эпикардальной жировой ткани: сравнение полуавтоматического измерения и алгоритма машинного обучения. <i>Кардиология</i> . 2020;60(9):46–54].
<i>Corresponding author</i>	Chernina V. Yu. E-mail: chernina909@gmail.com

Epicardial adipose tissue (EAT) is located between the myocardium and the visceral pericardium and is hormonally active [1]. In addition to preadipocytes and adipocytes, EAT contains stromovascular cells, immune cells, and macrophages [2] which can secrete pro-inflammatory cytokines, such as tumor necrosis factor alpha (TNFα), interleukin (IL) 1 beta, IL-6, and monocyte chemoattractant protein-1 (MCP-1) which can cause an inflammatory reaction, endothelial and smooth muscle cell

proliferation, atherogenesis, and destabilization of atherosclerotic plaque [3, 4]. Several trials, including a large multinational, randomized trial on atherosclerosis MESA (Multi-Ethnic Study of Atherosclerosis), have shown that EAT is an independent predictor of coronary artery disease (CAD) [5–9].

The possibility of evaluating this predictor in preclinical CAD is of the greatest interest. EAT can be evaluated using echocardiogram, computed tomography (CT), and magnetic

resonance imaging (MRI). The echocardiogram method is not the best method for quantifying EAT due to its low reproducibility, especially within a poor acoustic window and uneven distribution of fat around the heart [10]. Cardiac MRI is a very expensive and time-consuming examination, thus rendering it impossible to use it as a screening method [11].

CT (manual, semi-automatic, and automatic techniques) can measure EAT volume to high precision [12–15]. Manual and semi-automatic techniques are time-consuming, which prevents their routine use.

A pilot project has been ongoing in Moscow since 2017. In this project low-dose computed tomography (LDCT) of the chest is used for the screening of lung cancer. Unique screening protocols have been developed to perform qualitative CT of the chest, in order to detect lung lesions using a radiation dose of less than 1 mSv [16]. The LDCT evaluation of EAT volumes used in the screening project can identify asymptomatic patients [17].

## Objective

To compare the EAT volume evaluation results obtained by a semi-automatic machine-learning algorithm of the analysis performed by physicians and automatic algorithm based on the LDCT and standard chest CT findings.

## Material and Methods

The study was conducted following the Declaration of Helsinki. The independent ethics committee approved the protocol of this retrospective study. It was decided that there was no need for informed consent of the subjects (or their guardians).

Between January 2019 and May 2019, this analytical retrospective cross-sectional study randomly included 100 patients from the unified radiological information service (ERIS) database. Of these patients, 47 were male, and 53 were female (mean age  $60.7 \pm 9.4$  years). They underwent chest LDCT within project Low-Dose Computed Tomography of Chest as a Screening Method for the Diagnosis of Lung Cancer and other Chest Organ Diseases ( $n=50$ ) and chest CT according to the standard protocol ( $n=50$ ) in the outpatient clinics of Moscow.

This study included patients who met all of the following criteria: age from 50 to 75; smoked more than 20 pack-years; no neoplasm symptoms and corresponding complaints (except for smoking-related symptoms: cough, sputum, shortness of breath). Patients were excluded from the study, if they met any of the following criteria: supervision of an oncologist for lung tumor; less than 1 year since the previous chest CT; had quit smoking more than 10 years previously; less than 1 month after recovery from respiratory disease; any of the following symptoms at the time of the study: chest pain,

body temperature above  $37.5^{\circ}\text{C}$ , coughing up blood or pink sputum, unexplained weight loss in the past month or more, and hoarseness.

Two radiologists evaluated every examination and an artificial intelligence algorithm was used to facilitate evaluation of the EAT volume completely automatically (Figure 1).

Chest LDCT was performed on Toshiba Aquillion 64 CT scanners using special low-dose protocols for a patient of different weights (up to 69 kg, 70–89 kg, over 90 kg): tube voltage 135 kV, tube current 15–25 mA (depending on body weight), rotation time 0.50 s, pitch 1.484, slice thickness 1 mm. All examinations were performed using a dose of 1 mSv.

Chest CT was performed on Toshiba Aquillion 64 CT scanners following the standard protocol: tube voltage 120 kV, tube current 50 mA, rotation time 0.50 s, pitch 0.938, slice thickness 1 mm.

The Syngo.via VB20 workstation was used to map the pericardial contour in each examination manually. The EAT volume was automatically calculated, taking into account all voxels inside the pericardial contour within the density thresholds from  $-190$  HU to  $-50$  HU. Each examination was evaluated by two radiologists with more than two years of experience. The radiologists were unable to see each others' mapping.

Every examination was evaluated using an artificial intelligence algorithm that allows automatic evaluation of the EAT volume.

## Statistical Analysis

Descriptive statistics methods were used for statistical analysis. A paired t-test was used to compare volume measurements carried out using different methods. Correlation analysis was performed with the indication of Pearson's correlation coefficient and corresponding p-value. The t-test was used to compare the volume differences between different methods, CT and LDCT. Regression analysis was used to evaluate the correlation between different factors and the volume difference obtained by different physicians. The two-tailed significance level  $p=0.05$  was used in the statistical analysis. The analysis was performed using the Stata14 software.

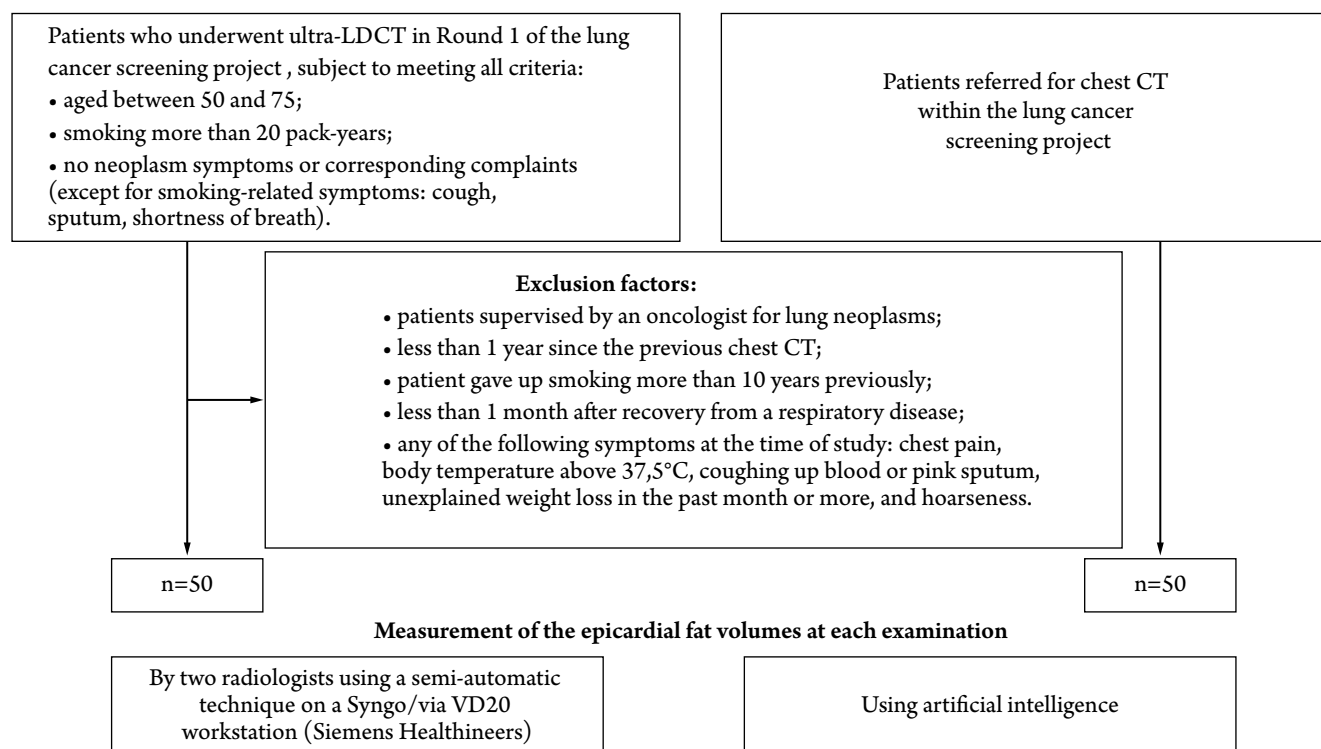
## Results

### Artificial intelligence

The model of the development of an artificial intelligence algorithm for the automatic measurement of EAT volume is shown in Figure 1.

The following steps were taken to evaluate EAT volume: localizing slices within the anatomical limits of interest and estimating the center point of the pericardial contour for each of them (1a), transferring to cylindrical coordinates (1b), building the pericardial curve in cylindrical coordinates

**Figure 1.** Design of this study with inclusion and exclusion criteria



LDCT, low-dose computed tomography; CI, confidence interval.

(2a); transferring to the original coordinates and estimating the EAT volume using the pericardial contour detected (2b).

The algorithm was trained on 352 chest LDCT examinations and 97 chest CT examinations. Two radiologists pre-mapped the pericardial contours for each examination; the third expert refined the contour in case of significant differences between the radiologists. The algorithm was then validated on 88 chest LDCT and 25 chest CT scans. The process of developing an artificial intelligence algorithm included two main steps. The first step was trained by means of assessing on each axial slice whether the selected slice was within the range of interest from the right pulmonary artery origin from the main pulmonary artery to the diaphragm, with a search for a geometric center of the pericardial contour in the appropriate slices. The general method architecture is based on a 3D convolutional network [18] and is similar to the work of Pisov et al. by definition of the brain midline shift [19]. At the second step of the algorithm, the centers detected were used to transfer to the cylindrical coordinates which had already been used by Commandeur et al. [20]. The second convolutional network was also based on the approach used to determine the brain midline shift [19]. However, the pericardial curve of interest was defined in the entire image in this study, while the standard second network output was not used. It should be noted that the method used in our study guarantees the continuity of the pericardial contour.

### Comparison of consistency between physicians' measurements

There was a 98.4% ( $p < 0.0001$ ) correlation coefficient between the radiologists' evaluations (physician 1 and physician 2) of the EAT volumes (Table 1). Volume differences did not exceed the mean of 8 mL (5%).

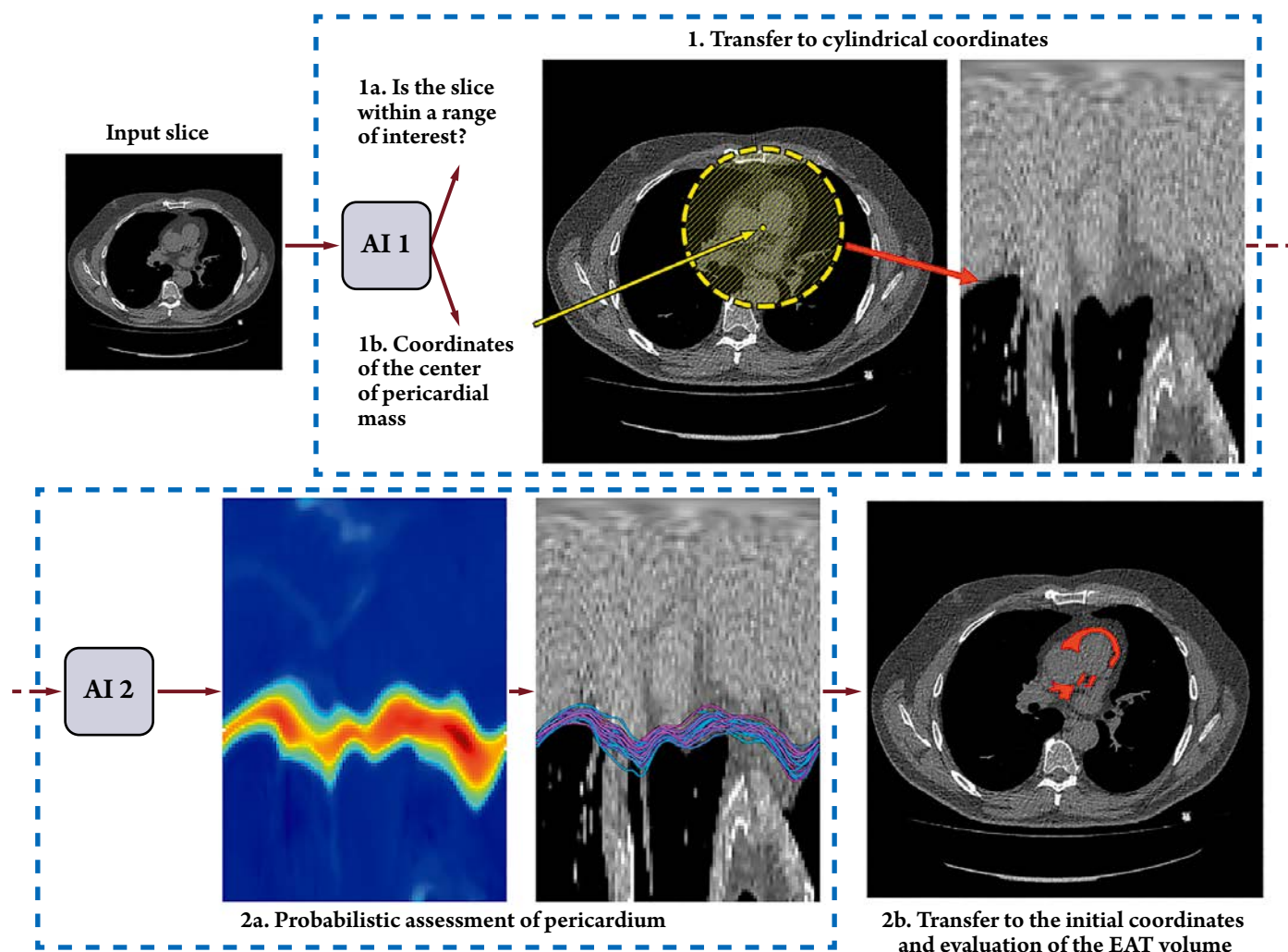
### Comparison of the consistency between physicians' measurements and artificial intelligence

The correlation coefficient of EAT volumes between artificial intelligence and physician 1 was 95.8%. The correlation coefficient of EAT volumes between artificial intelligence and physician 2 was 95.8%. Differences in EAT volumes in the comparisons with physician 1 and physician 2 did not exceed the mean of 8 mL.

The correlation coefficient between the LDCT evaluations of artificial intelligence and physician 1 and physician 2 was 94.2% and 95.0%, respectively ( $p < 0.0001$ ). The correlation coefficient between the CT evaluations of artificial intelligence and physician 1 and physician 2 was 97.0% and 95.8%, respectively ( $p < 0.0001$ ).

Evaluation of the difference in EAT volume measurements using artificial intelligence is shown in Figure 3. Examples of automatic EAT mapping using the artificial intelligence algorithm based on chest CT and LDCT are shown in Figure 4 and Figure 5, respectively.

**Figure 2.** Development an artificial intelligence model for the automatic EAT volume measurement



The yellow arrow indicates the estimated center of the pericardial mass on a chest CT slice. The red arrow shows a hatched circle transferred into a cylindrical coordinate system. See detailed explanation in the text. AI, artificial intelligence; EAT, epicardial adipose tissue.

A comparison of the difference of the epicardial adipose tissue volumes measures by CT and LDCT is provided in Table 2.

#### *Evaluation of the effect of noise level on the consistency between physicians' measurements*

The analysis of the noise level effect on the consistency between physicians' measurements showed that a regression coefficient close to 0 and was not statistically significant ( $p=0.855$ ; Table 3).

#### *Time of measurement of the epicardial fat tissue volume*

It took a physician  $17\pm 3$  minutes to map and evaluate the EAT volume of one LDCT examination. It took  $14\pm 3$  minutes to evaluate the EAT volume using the semi-automatic technique.

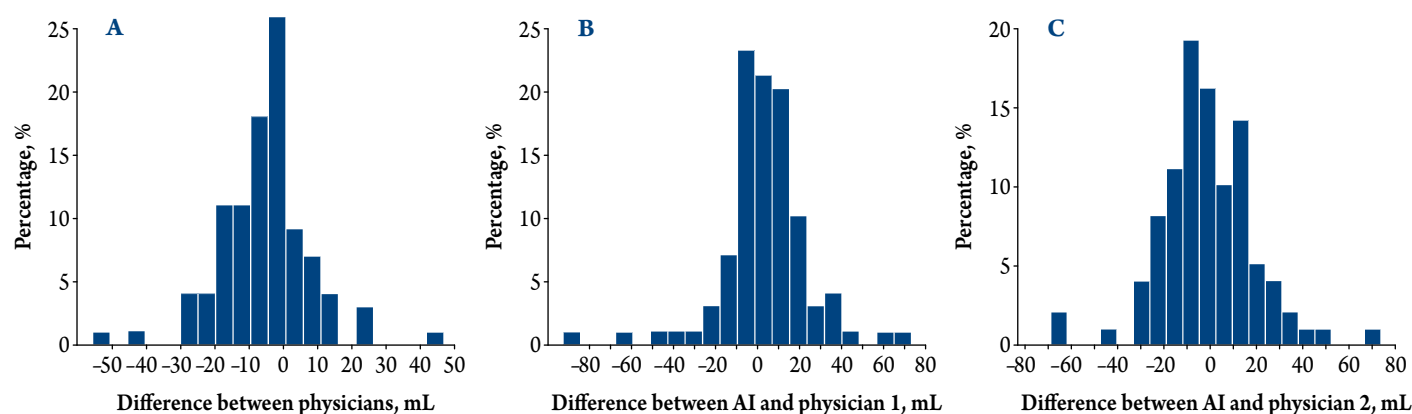
**Table 1.** Comparison of volumes (mL) of epicardial adipose tissue measured by two physicians

Parameter	Physician 1	Physician 2	Difference between scores of Physicians 1 and 2
Number of studies	100	100	100
Mean	150.07	144.99	-5.07
SD	74.74	71.73	13.43
95% CI	(from 135.24 to 164.90)	(from 130.76 to 159.22)	(from -7.74 to -2.41)
Min	34.32	40.94	-55.41
Max	354.98	345.99	47.00
Med	133.11	128.96	-4.22
p (paired t-test)	-	-	0.0003

CI, confidence interval; SD, standard deviation.



**Figure 3.** Evaluation of the difference in the measurement of epicardial fat tissue volumes between artificial intelligence and physicians 1 and 2



A – semi-automatic measurements, between physicians 1 and 2; B – between the artificial intelligence and semi-automatic measurement made by physician 1; C – between the artificial intelligence and semi-automatic measurement made by physician 2. AI, artificial intelligence.

The segmentation and volume measurement of a single examination (LDCT or CT) took  $38 \pm 2$  seconds using artificial intelligence.

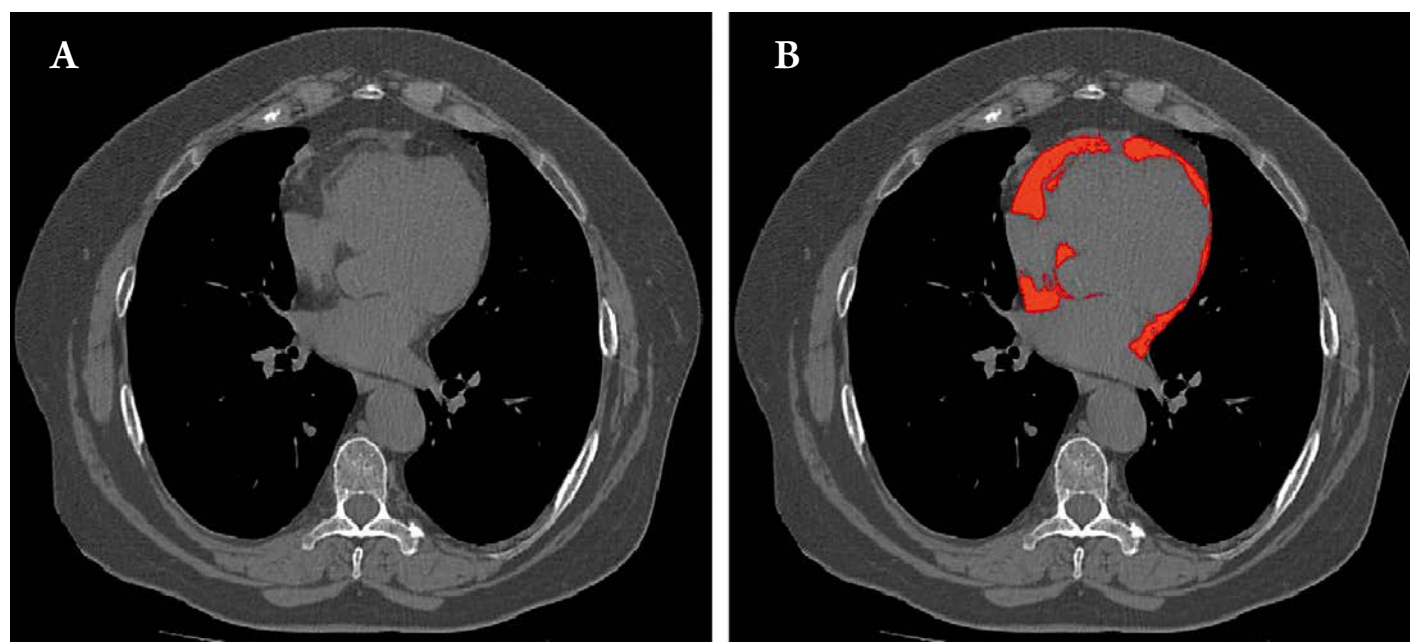
## Discussion

The comparison of chest LDCT and CT measurement of the EAT volume showed high consistency of results both in the expert semi-automatic analysis, and between expert mapping and artificial intelligence.

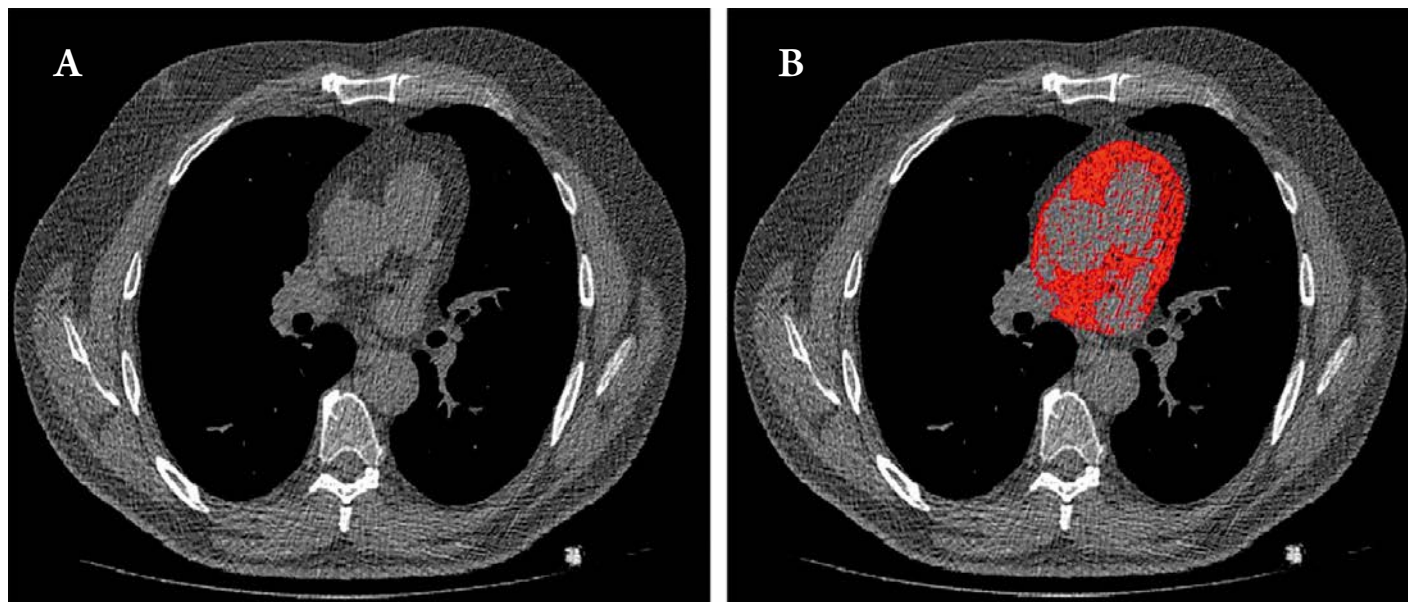
The EAT evaluation algorithm is based on supervised machine learning methods. An integral part of such approaches is a learning sample consisting of the input-output pairs. Training involves the automatic search for a

mathematical formula (sometimes extremely complex with millions of parameters) that would allow estimation of the output data from the input set [21]. Such approaches have been in development for over half a century but have primarily been aimed at processing simple input data (for example, several quantitative variables). The past decade has seen a breakthrough in automated image analysis thanks to the development of deep convolutional network-based methods. The key idea is a hierarchic search for such numerical characteristics extracted from an image which would allow the construction of an estimate of the output data in the best way [22]. Specialized techniques based on convolutional networks have also gone further in analyzing medical images, primarily

**Figure 4.** Example of automatic artificial intelligence mapping of epicardial fat tissue based on chest CT data



A – axial scan of the chest CT; B – automatic mapping of epicardial fat tissue on the same axial chest CT scan (red).

**Figure 5.** Example of automatic artificial intelligence mapping of epicardial fat tissue based on chest LDCT data**A** – axial scan of the chest LDCT; **B** – automatic marking of epicardial fat tissue on the same axial chest LDCT scan (red).**Table 2.** Comparison of the difference of epicardial adipose tissue volumes measures by CT and LDCT

Comparison	Difference (95% CI)	p (t-test)	Correlation coefficient		
			Total CT and LDCT	CT	LDCT
Between physicians' measurements	1.27 (from -4.08 to 6.62)	0.639	0.984	0.987	0.979
Between the algorithm and measurements of Physician 1	8.53 (from 0.37 to 16.70)	0.0407	0.958	0.970	0.942
Between the algorithm and measurements of Physician 2	9.08 (from 1.07 to 17.09)	0.0268	0.958	0.958	0.950

LDCT, low-dose computed tomography; CI, confidence interval.

**Table 3.** Parameters of the multivariate regression model for differences in epicardial fat volume measured by two physicians

Model factor	Regression coefficient	p	95% CI
Noise level per STD unit	-0.008	0.855	(from -0.093 to 0.077)
Examination type (CT=ref)	-1.58	0.641	(from -8.31 to 5.14)
Age, per year	-0.19	0.213	(from -0.48 to 10.8)
Sex (female=ref)	-3.56	0.195	(from -8.97 to 1.85)
Intercept	9.33	0.353	(from -10.5 to 29.16)

CI, confidence interval; STD, standard deviation.

stratification of patients by groups and mapping pathological lesions [23]. Convolutional networks can also be used to create an algorithm for the automatic evaluation of EAT volume. In this case, CT or LDCT images will be used as input data for training, and a series of axial slices with pericardial contours will be used as output data.

Automatic segmentation and volume measurement take 40 seconds or less in a single study. This is 30 times faster than expert quantification and potentially facilitates the clinical quantification of EAT volume.

This study did not show any statistically significant differences between the volumes measured by physicians and

the algorithm. However, it is worth noting that the prediction for the LDCT images was statistically significantly more accurate than for the CT images. This is because the initial algorithm was based on a sample consisting mainly of LDCT data (78% LDCT and 22% CT examinations).

Several studies, including a systematic review, have shown a threshold EAT volume of 125 mL [8, 9, 24]. According to world literature, EAT volume has never been measured based on chest LDCT data. In 2018, Commandeur et al. [14] introduced an algorithm which allowed for estimation of EAT volume based on ECG-gated non-contrast-enhanced CT (convolutional neural network, ConvNet). ECG-gated non-

contrast-enhanced CT was used to evaluate model accuracy in 250 patients. The correlation coefficient was 0.97 between the expert scores and 0.98 between the expert scores and the algorithm. These results are comparable to ours. Moreover, our algorithm allows for accurate estimation of EAT volume based on the LDCT data without ECG gating which allows us to propose it for lung cancer screening.

All LDCT examinations were conducted with a dose of less than 1 mSv, which meets the criteria for preventive X-ray studies in adults (SanPiN 2.6.1.1192–03) and 2020 guidelines of the European Lung Cancer Screening Consortium [25].

Due to the limited exposure dose, chest LDCT images are noisier than the standard CT images. This may have affected the quality of manual mapping of the pericardium by physicians based on the LDCT data, and therefore the resulting EAT volumes. However, this study showed no correlation between the physicians' measurements of the EAT volumes and the noise levels in the images.

In another recent study, a close correlation was found between EAT volumes evaluated using CT coronary angiography and non-ECG gated CT ( $r=0.948$ ;  $p<0.001$ ) [26]. The comparability of EAT volumes as measured by LDCT and

CT coronary angiography is still under question. Work will continue in this area.

### Limitations

Expert and machine mapping was compared in a relatively small sample. We plan to assess the artificial intelligence algorithm based on significantly more data. Noise level is higher in ultra-LDCT than in standard chest CT examinations. This is why when evaluating volume, the algorithm takes additional pixels into account. The issue will be addressed in the next stage.

### Conclusion

The results on the comparability of epicardial fat volumes measured by semi-automatic and automatic techniques suggest that the artificial intelligence algorithm will contribute to the faster analysis of cardiac fat and improve stratification of the cardiovascular complication risk without additional patient exposure.

*No conflict of interest is reported.*

**The article was received on 15/03/2020**

### REFERENCES

1. Drapkina O.M., Korneeva O.N., Drapkina Yu.S. Epicardial fat: a striker or a spare? Rational Pharmacotherapy in Cardiology. 2013;9(3):287–91. [Russian: Драпкина О.М., Корнеева О.Н., Драпкина Ю.С. Эпикардальный жир: нападающий или запасной? Рациональная фармакотерапия в кардиологии. 2013;9(3):287–91]. DOI: 10.20996/1819-6446-2013-9-3-287-291
2. Iacobellis G. Local and systemic effects of the multifaceted epicardial adipose tissue depot. Nature Reviews Endocrinology. 2015;11(6):363–71. DOI: 10.1038/nrendo.2015.58
3. Karmazyn M, Purdham DM, Rajapurohitam V, Zeidan A. Signalling mechanisms underlying the metabolic and other effects of adipokines on the heart. Cardiovascular Research. 2008;79(2):279–86. DOI: 10.1093/cvr/cvn115
4. Patel VB, Shah S, Verma S, Oudit GY. Epicardial adipose tissue as a metabolic transducer: role in heart failure and coronary artery disease. Heart Failure Reviews. 2017;22(6):889–902. DOI: 10.1007/s10741-017-9644-1
5. Ding J, Hsu F-C, Harris TB, Liu Y, Kritchevsky SB, Szklo M et al. The association of pericardial fat with incident coronary heart disease: the Multi-Ethnic Study of Atherosclerosis (MESA). The American Journal of Clinical Nutrition. 2009;90(3):499–504. DOI: 10.3945/ajcn.2008.27358
6. Britton KA, Massaro JM, Murabito JM, Kreger BE, Hoffmann U, Fox CS. Body Fat Distribution, Incident Cardiovascular Disease, Cancer, and All-Cause Mortality. Journal of the American College of Cardiology. 2013;62(10):921–5. DOI: 10.1016/j.jacc.2013.06.027
7. Mahabadi AA, Berg MH, Lehmann N, Kälsch H, Bauer M, Kara K et al. Association of Epicardial Fat With Cardiovascular Risk Factors and Incident Myocardial Infarction in the General Population. Journal of the American College of Cardiology. 2013;61(13):1388–95. DOI: 10.1016/j.jacc.2012.11.062
8. Forouzandeh F, Chang SM, Muhyieddeen K, Zaid RR, Trevino AR, Xu J et al. Does Quantifying Epicardial and Intrathoracic Fat With Noncontrast Computed Tomography Improve Risk Stratification Beyond Calcium Scoring Alone? Circulation: Cardiovascular Imaging. 2013;6(1):58–66. DOI: 10.1161/CIRCIMAGING.112.976316
9. Cheng VY, Dey D, Tamarappoo B, Nakazato R, Gransar H, Miranda-Peats R et al. Pericardial Fat Burden on ECG-Gated Noncontrast CT in Asymptomatic Patients Who Subsequently Experience Adverse Cardiovascular Events. JACC: Cardiovascular Imaging. 2010;3(4):352–60. DOI: 10.1016/j.jcmg.2009.12.013
10. Kim BJ, Kang JG, Lee SH, Lee JY, Sung KC, Kim BS et al. Relationship of Echocardiographic Epicardial Fat Thickness and Epicardial Fat Volume by Computed Tomography with Coronary Artery Calcification: Data from the CAESAR Study. Archives of Medical Research. 2017;48(4):352–9. DOI: 10.1016/j.arcmed.2017.06.010
11. Flächter S, Haghi D, Dinter D, Heberlein W, Kühl HP, Neff W et al. Volumetric Assessment of Epicardial Adipose Tissue With Cardiovascular Magnetic Resonance Imaging. Obesity. 2007;15(4):870–8. DOI: 10.1038/oby.2007.591
12. Lim C, Ahn M-I, Jung JI, Beck KS. Simple quantification of paracardial and epicardial fat dimensions at low-dose chest CT: correlation with metabolic risk factors and usefulness in predicting metabolic syndrome. Japanese Journal of Radiology. 2018;36(9):528–36. DOI: 10.1007/s11604-018-0752-1
13. Miyazawa I, Ohkubo T, Kadowaki S, Fujiyoshi A, Hisamatsu T, Kadohira A et al. Change in Pericardial Fat Volume and Cardiovascular Risk Factors in a General Population of Japanese Men. Circulation Journal. 2018;82(10):2542–8. DOI: 10.1253/circj.CJ-18-0153
14. Commandeur F, Goeller M, Betancur J, Cadet S, Doris M, Chen X et al. Deep Learning for Quantification of Epicardial and Thoracic Adipose Tissue From Non-Contrast CT. IEEE Transactions on Medical Imaging. 2018;37(8):1835–46. DOI: 10.1109/TMI.2018.2804799
15. Chernina V.Yu., Morozov S.P., Nizovtsova L.A., Blokhin I.A., Sitdikov D.I., Gomboleviskiy V.A. The Role of Quantitative Assessment of Visceral Adipose Tissue of the Heart as a Predictor for Cardiovascular Events. Journal of radiology and nuclear medicine. 2020;100(6):387–94. [Russian: Чернина В.Ю., Морозов С.П., Низовцова Л.А., Блохин И.А., Ситдигов Д.И., Гомболевский В.А. Роль количественной оценки висцеральной жировой ткани сердца как предиктора развития сердечно-сосудистых событий. Вест-





# ФОРСИГА® — НОВЫЙ ЖИЗНЕСПАСАЮЩИЙ ПРЕПАРАТ ДЛЯ ПАЦИЕНТОВ С ХСН<sub>н</sub>ФВ<sup>1, #</sup>

## СОХРАНИТЬ САМУ ЖИЗНЬ

↓ **26%**

Снижает риск СС смерти и госпитализаций по поводу СН\*<sup>4</sup>

### УДОБСТВО:

1 таблетка  
10 мг<sup>1</sup>



1 раз  
в сутки<sup>1</sup>



без  
титрации<sup>1</sup>

**! ВКЛЮЧЕН В ЖНВЛП<sup>2</sup> И ОНЛС<sup>3</sup>**

**КРАТКАЯ ИНСТРУКЦИЯ ПО МЕДИЦИНСКОМУ ПРИМЕНЕНИЮ ЛЕКАРСТВЕННОГО ПРЕПАРАТА ФОРСИГА®. РЕГИСТРАЦИОННЫЙ НОМЕР: ЛП-002596. ТОРГОВОЕ НАЗВАНИЕ: ФОРСИГА (FORSIGA)®. МЕЖДУНАРОДНОЕ НЕПАТЕНТОВАННОЕ НАЗВАНИЕ: ДАПАГЛИФЛОЗИН. ЛЕКАРСТВЕННАЯ ФОРМА: таблетки, покрытые пленочной оболочкой. ПОКАЗАНИЯ К ПРИМЕНЕНИЮ: САХАРНЫЙ ДИАБЕТ 2 ТИПА** у взрослых пациентов в дополнение к диете и физическим упражнениям для улучшения гликемического контроля в качестве: монотерапии, когда применение метформина невозможно ввиду непереносимости; комбинированной терапии с метформин, производными сульфонилмочевины (в том числе, в комбинации с метформин), тиазолидинонами, ингибиторами дипептидилпептидазы 4 (ДПП-4) (в том числе, в комбинации с метформин); агонистом рецепторов глуканогоподобного полипептида-1 (ГПП-1) экстендидом пролонгированного действия в комбинации с метформин; препаратом инсулина (в том числе, в комбинации с одним или двумя гипогликемическими препаратами для перорального применения) при отсутствии адекватного гликемического контроля на данной терапии; стартовой комбинированной терапии с метформин, при целесообразности данной терапии. Сахарный диабет 2 типа у взрослых пациентов с установленным диагнозом сердечно-сосудистого заболевания или двумя и более факторами сердечно-сосудистого риска (возраст у мужчин  $\geq 55$  лет или  $\geq 60$  лет у женщин и наличие не менее одного фактора риска: дислипидемия, артериальная гипертензия, курение) для снижения риска госпитализации по поводу сердечной недостаточности. **СЕРДЕЧНАЯ НЕДОСТАТОЧНОСТЬ. ЦЕЛЬ: ОН-ИВ функциональный класс по классификации NYHA) со сниженной фракцией выброса у взрослых пациентов для снижения риска сердечно-сосудистой смерти и госпитализации по поводу сердечной недостаточности. ПРОТИВОПОКАЗАНИЯ:** повышенная индивидуальная чувствительность к любому компоненту препарата; сахарный диабет 1-го типа; диабетический кетоацидоз; нарушение функции почек при расчетной СКФ (рСКФ) стабильно менее 45 мл/мин/1,73 м<sup>2</sup>, включая нарушение функции почек тяжелой степени и терминальную стадию почечной недостаточности; при применении по показаниям «сердечная недостаточность» (в связи с ограниченным опытом применения в клинических исследованиях); наследственная непереносимость лактозы, дефицит лактазы или глюкозо-галактозная мальабсорбция; беременность и период грудного вскармливания; детский возраст до 18 лет (безопасность и эффективность не изучены). **ОСТОРОЖНОСТЬ:** печеночная недостаточность тяжелой степени, инфекции мочевыводящей системы, повышенное значение гематокрита. **ПРИМЕНЕНИЕ В ПЕРИОД БЕРЕМЕННОСТИ И ГРУДНОГО ВСКАРМЛИВАНИЯ** в связи с тем, что применение дапаглифлозина в период беременности не изучено, препарат противопоказан в период беременности. В случае диагностирования беременности терапия дапаглифлозином должна быть прекращена. Неизвестно, проникает ли дапаглифлозин и/или его неактивные метаболиты в грудное молоко. Нельзя исключать риск для новорожденных/младенцев. **СПОСОБ ПРИМЕНЕНИЯ И ДОЗЫ:** Внутрь, независимо от приема пищи, не разжевывая. Сахарный диабет 2 типа. Мониторинг: рекомендуемая доза препарата Форсига составляет 10 мг один раз в сутки. Комбинированная терапия: рекомендуемая доза препарата Форсига составляет 10 мг один раз в сутки в комбинации с метформин, производными сульфонилмочевины (в том числе, в комбинации с метформин), тиазолидинонами, ингибиторами ДПП-4 (в том числе, в комбинации с метформин); агонистом рецепторов ГПП-1 — экстендидом пролонгированного действия, в комбинации с метформин; препаратами инсулина (в том числе, в комбинации с одним или двумя гипогликемическими препаратами для перорального применения). С целью снижения риска гипогликемии при совместном назначении препарата Форсига с препаратами инсулина или препаратами, повышающими секрецию инсулина (например, с производными сульфонилмочевины), может потребоваться снижение дозы препаратов инсулина или препаратов, повышающих секрецию инсулина. Стартовая комбинированная терапия с метформин: рекомендуемая доза препарата Форсига составляет 10 мг один раз в сутки, доза метформина — 500 мг один раз в сутки. В случае неадекватного гликемического контроля дозу метформина следует увеличить. СД2 у взрослых пациентов с установленным диагнозом сердечно-сосудистого заболевания или двумя и более факторами сердечно-сосудистого риска для снижения риска госпитализации по поводу сердечной недостаточности: рекомендуемая доза препарата Форсига составляет 10 мг один раз в сутки. **Сердечная недостаточность: рекомендуемая доза препарата Форсига составляет 10 мг один раз в сутки. ПОБОЧНОЕ ДЕЙСТВИЕ.** Крайний обзор профиля безопасности. В клинических исследованиях СД2 более 15000 пациентов получали терапию дапаглифлозином. Первичная оценка безопасности и переносимости проводилась в заранее запланированном анализе объединенных данных 13 краткосрочных (до 24 недель) плацебо-контролируемых исследований, в которых 2560 пациентов принимали дапаглифлозин в дозе 10 мг и 2295 пациентов получали плацебо. В исследовании дапаглифлозина в отношении сердечно-сосудистых исходов при СД2 (DECLARE) 8574 пациента получали дапаглифлозин 10 мг и 8569 получали плацебо (медиана воздействия 48 месяцев). В общей сложности экспозиция дапаглифлозином составила 30623 пациент-лет. В исследовании дапаглифлозина в отношении сердечно-сосудистых исходов у пациентов с сердечной недостаточностью со сниженной фракцией выброса (DAPA-HF) 2368 пациентов получали дапаглифлозин 10 мг и 2368 получали плацебо (медиана воздействия 18 месяцев). Популяция включала пациентов с СД2 и без него, и пациентов с рСКФ  $\geq 30$  мл/мин/1,73 м<sup>2</sup>. Профиль безопасности дапаглифлозина в исследовании был в целом схожим по изучаемым показателям. Тяжелую гипогликемию и диабетический кетоацидоз отмечали только у пациентов с сахарным диабетом. Ниже представлены НР, отмечавшиеся в плацебо-контролируемых клинических исследованиях и при пострегистрационном применении. Ни одна из них не зависела от дозы препарата. НР классифицированы по частоте и классу систем и органов. Частота НР представлена в виде следующей градации: очень часто ( $\geq 1/10$ ), часто ( $\geq 1/100$ ,  $< 1/10$ ), нечасто ( $\geq 1/1000$ ,  $< 1/100$ ), редко ( $\geq 1/10000$ ,  $< 1/1000$ ), очень редко ( $< 1/10000$ ) и неучтенной частоты (невозможно оценить по полученным данным). Инфекционные и паразитарные заболевания: часто — вульвовагинит, баланит и связанные с ними генитальные инфекции, инфекция мочевыводящих путей; нечасто — вульвовагинальный зуд, грибковые инфекционные заболевания; очень редко — некротизирующий фасциит промежности (гайгана Фурье). Нарушения со стороны обмена веществ и питания: очень часто — гипогликемия (при применении в комбинации с производными сульфонилмочевины или инсулином); нечасто — диабетический кетоацидоз (при применении при СД2). Нарушения со стороны нервной системы: часто — головкружение. Нарушения со стороны желудочно-кишечного тракта: нечасто — запор, сухость во рту. Нарушения со стороны кожи и подкожных тканей: часто — сыпь, очень редко — ангионевротический отек. Нарушения со стороны костно-мышечной системы и соединительной ткани: часто — боль в спине. Нарушения со стороны почек и мочевыводящих путей: часто — дисурия, полиурия; нечасто — неустойчивость. Лабораторные и инструментальные данные: часто — дислипидемия, повышение значения гематокрита, снижение почечного клиренса креатинина на начальном этапе терапии; нечасто — повышение концентрации мочевины в крови, повышение концентрации креатинина в крови на начальном этапе терапии.

Ссылка на полную инструкцию: Инструкция по медицинскому применению лекарственного препарата Форсига® (таблетки, покрытые пленочной оболочкой, 5 мг, 10 мг). Регистрационное удостоверение ЛП-002596 от 21.08.2014

ХСН<sub>н</sub>ФВ — хроническая сердечная недостаточность со сниженной фракцией выброса; СС — сердечно-сосудистый; СН — сердечная недостаточность.

\* Включая неотложные обращения по причине СН. <sup>#</sup> Снижение относительного риска сердечно-сосудистой смерти и смерти от всех причин в группе дапаглифлозина по сравнению с плацебо в исследовании DAPA-HF.

1. Инструкция по медицинскому применению лекарственного препарата Форсига® (таблетки, покрытые пленочной оболочкой, 5 мг, 10 мг). Регистрационное удостоверение ЛП-002596 от 21.08.2014.

2. Перечень жизненно необходимых и важнейших лекарственных препаратов для медицинского применения 3. Перечень лекарств для обеспечения отдельных категорий граждан. 4. McMurtry JJV et al., N Engl J Med. 2019;381(21):1995-2008.

Информация предназначена для специалистов здравоохранения. Имеются противопоказания. Перед назначением ознакомьтесь, пожалуйста, с полной инструкцией по медицинскому применению лекарственного препарата. ООО «АстраЗенка Фармасьютикалс», 123112, Москва, Ч/Я Красногвардейский проезд, д.21, стр.1, 30 этаж бизнес-центр «МО». Тел: +7 (495) 799-56-99, факс: +7 (495) 799-56-98 www.astrazeneca.ru

FOR-RU-7882. Дата одобрения: 24.07.2020. Дата истечения: 23.07.2022.

AstraZeneca



- ник рентгенологии и радиологии. 2019;100(6):387-94]. DOI: 10.20862/0042-4676-2019-100-6-387-394
16. Morozov S.P., Kuzmina E.S., Vetsheva N.N., Gombolevskiy V.A., Lantukh Z.A., Polishuk N.S. et al. Moscow Screening: Lung Cancer Screening With Low-Dose Computed Tomography. Problems of Social Hygiene Public Health and History of Medicine. 2019;27(S):630–6. [Russian: Морозов С.П., Кузьмина Е.С., Ветшева Н.Н., Гомболевский В.А., Лантух З.А., Полищук Н.С. и др. Московский скрининг: скрининг рака легкого с помощью низкодозовой компьютерной томографии. Проблемы социальной гигиены, здравоохранения и истории медицины. 2019;27(S):630–6]. DOI: 10.32687/0869-866X-2019-27-si1-630-636
17. Nikolaev A.E., Gombolevskiy V.A., Gonchar A.P., Shapiev A.N., Laypan A.Sh., Morozov S.P. Incidental findings during lung cancer screening by low-dose computed tomography. Tuberculosis and lung diseases. 2018;96(11):60–7. [Russian: Николаев А.Е., Гомболевский В.А., Гончар А.П., Шапиев А.Н., Лайпан А.Ш., Морозов С.П. Случайные находки при скрининге рака легкого методом низкодозной компьютерной томографии. Туберкулез и болезни легких. 2018;96(11):60-7]. DOI: 10.21292/2075-1230-2018-96-11-60-67
18. Milletari F, Navab N, Ahmadi S-A. V-Net: Fully Convolutional Neural Networks for Volumetric Medical Image Segmentation. 2016 Fourth International Conference on 3D Vision (3DV). P. 565–571. 2016. [DOI: 10.1109/3DV.2016.79]
19. Pisov M, Goncharov M, Kurochkina N, Morozov S, Gombolevskiy V, Chernina V et al. Correction to: Incorporating Task-Specific Structural Knowledge into CNNs for Brain Midline Shift Detection. Series Title: Lecture Notes in Computer Science. [DOI: 10.1007/978-3-030-33850-3\_11]. In: Interpretability of Machine Intelligence in Medical Image Computing and Multimodal Learning for Clinical Decision Support ETH Zurich, Suzuki K, Reyes M, Syeda-Mahmood T, Glocker B, Wiest R, et al., editors -Cham: Springer International Publishing;2020.
20. Commandeur F, Goeller M, Razipour A, Cadet S, Hell MM, Kwicinski J et al. Fully Automated CT Quantification of Epicardial Adipose Tissue by Deep Learning: A Multicenter Study. Radiology: Artificial Intelligence. 2019;1(6):e190045. DOI: 10.1148/ryai.2019190045
21. Deo RC. Machine Learning in Medicine. Circulation. 2015;132(20):1920–30. DOI: 10.1161/CIRCULATIONAHA.115.001593
22. LeCun Y, Bengio Y, Hinton G. Deep learning. Nature. 2015;521(7553):436–44. DOI: 10.1038/nature14539
23. Greenspan H, van Ginneken B, Summers RM. Guest Editorial Deep Learning in Medical Imaging: Overview and Future Promise of an Exciting New Technique. IEEE Transactions on Medical Imaging. 2016;35(5):1153–9. DOI: 10.1109/TMI.2016.2553401
24. Spearman JV, Renker M, Schoepf UJ, Krazinski AW, Herbert TL, De Cecco CN et al. Prognostic value of epicardial fat volume measurements by computed tomography: a systematic review of the literature. European Radiology. 2015;25(11):3372–81. DOI: 10.1007/s00330-015-3765-5
25. Kauczor H-U, Baird A-M, Blum TG, Bonomo L, Bostantzoglou C, Burghuber O et al. ESR/ERS statement paper on lung cancer screening. European Radiology. 2020;30(6):3277–94. DOI: 10.1007/s00330-020-06727-7
26. Nagayama Y, Nakamura N, Itatani R, Oda S, Kusunoki S, Takahashi H et al. Epicardial fat volume measured on nongated chest CT is a predictor of coronary artery disease. European Radiology. 2019;29(7):3638–46. DOI: 10.1007/s00330-019-06079-x